Ciliopathy due to POC1A deficiency: clinical and metabolic features, and cellular modeling

Kevin Perge, Emilie Capel, Carine Villanueva, Jérémie Gautheron, Safiatou Diallo, Martine Auclair, Sophie Rondeau, Romain Morichon, Frédéric Brioude, Isabelle Jéru, et al.

European Journal of Endocrinology, 2024, **190**, 151–164
https://doi.org/10.1093/ejendo/lvae009
Advance access publication 20 January 2024
Original Research

Ciliopathy due to POC1A deficiency: clinical and metabolic features, and cellular modeling

Kevin Perge,[1,2,*†] Emilie Capel,[3,†] Carine Villanueva,[1] Jérémie Gautheron,[3] Safiatou Diallo,[3] Martine Auclair,[3] Sophie Rondeau,[4] Romain Morichon,[3,5] Frédéric Brioude,[3,6] Isabelle Jéru,[3,7] Massimiliamo Rossi,[8,9] Marc Nicolino,[1,2,‡] and Corinne Vigouroux[3,7,10,*‡]

[1]Pediatric Endocrinology, Diabetology and Metabolism Department, Femme Mère Enfant Hospital, Hospices Civils de Lyon, Bron F69500, France
[2]Claude Bernard University, Lyon 1, Lyon F69100, France
[3]Sorbonne University, Inserm U938, Saint-Antoine Research Centre, and Institute of Cardiometabolism and Nutrition, F75012 Paris, France
[4]Department of Molecular Biology, Assistance Publique-Hôpitaux de Paris, Necker Enfants Malades Hospital, Paris F75015, France
[5]Cytometry and Imagery platform Saint-Antoine (CISA), Inserm UMS30 Lumic, Paris F75012, France
[6]Department of Molecular Biology and Genetics, Assistance Publique-Hôpitaux de Paris, Armand Trousseau University Hospital, Paris F75012, France
[7]Department of Molecular Biology and Genetics, Assistance Publique-Hôpitaux de Paris, Saint-Antoine University Hospital, Paris F75012, France
[8]Genetics Department, Referral Center for Skeletal Dysplasias, Femme Mère Enfant Hospital, Hospices Civils de Lyon, Lyon F69500, France
[9]UMR5292, Lyon Neuroscience Research Center, INSERM U1028, CNRS, GENDEV Team, Bron F69500, France
[10]Department of Endocrinology, Diabetology and Reproductive Endocrinology, Assistance Publique-Hôpitaux de Paris, Saint-Antoine University Hospital, National Reference Center for Rare Diseases of Insulin Secretion and Insulin Sensitivity (PRISIS), Paris F75012, France

*Corresponding authors: Pediatric Endocrinology, Diabetology and Metabolism Department, Femme Mère Enfant Hospital, Hospices Civils de Lyon, 59 Boulevard Pinel, Bron 69677, France. Email: kevin.perge@chu-lyon.fr (K.P.); Sorbonne Université Médecine, Site Saint-Antoine, 27, rue Chaligny, Paris Cédex 12 75571, France. Email: corinne.vigouroux@inserm.fr (C.V.)

Abstract

Objective: SOFT syndrome (MIM#614813), denoting Short stature, Onychodysplasia, Facial dysmorphism, and hypoTrichosis, is a rare primordial dwarfism syndrome caused by biallelic variants in *POC1A*, encoding a centriolar protein. SOFT syndrome, characterized by severe growth failure of prenatal onset and dysmorphic features, was recently associated with insulin resistance. This study aims to further explore its endocrinological features and pathophysiological mechanisms.

Design/Methods: We present clinical, biochemical, and genetic features of 2 unrelated patients carrying biallelic pathogenic *POC1A* variants. Cellular models of the disease were generated using patients' fibroblasts and *POC1A*-deleted human adipose stem cells.

Results: Both patients present with clinical features of SOFT syndrome, along with hyperinsulinemia, diabetes or glucose intolerance, hypertriglyceridemia, liver steatosis, and central fat distribution. They also display resistance to the effects of IGF-1. Cellular studies show that the lack of POC1A protein expression impairs ciliogenesis and adipocyte differentiation, induces cellular senescence, and leads to resistance to insulin and IGF-1. An altered subcellular localization of insulin receptors and, to a lesser extent, IGF1 receptors could also contribute to resistance to insulin and IGF1.

Conclusions: Severe growth retardation, IGF-1 resistance, and centripetal fat repartition associated with insulin resistance-related metabolic abnormalities should be considered as typical features of SOFT syndrome caused by biallelic *POC1A* null variants. Adipocyte dysfunction and cellular senescence likely contribute to the metabolic consequences of *POC1A* deficiency. SOFT syndrome should be included within the group of monogenic ciliopathies with metabolic and adipose tissue involvement, which already encompasses Bardet-Biedl and Alström syndromes.

Keywords: ciliopathy, insulin resistance, IGF1 resistance, short stature, *POC1A*, SOFT syndrome, adipose stem cells, adipose tissue

Significance

This translational study shows that, in addition to severe growth retardation, adipose tissue involvement with central repartition of fat and resistance to insulin and IGF1 are features of SOFT syndrome linked to biallelic null variants in *POC1A*, encoding a centriolar protein. Using patients' fibroblasts and *POC1A*-deleted human adipose stem cells, we show that *POC1A* deficiency is associated with abnormal cellular organization of cilia, impaired adipocyte differentiation, accelerated cellular senescence, and results in resistance to insulin and IGF1. A decrease amount of insulin receptors, and, to a lesser extent, of IGF1 receptors at the plasma membrane could also play a role. SOFT syndrome should be added to the group of monogenic ciliopathies with metabolic alterations and adipose tissue involvement.

† K.P. and E.C. contributed equally as co-first authors.
‡ M.N. and C.V. contributed equally as co-last authors.

Received: September 30, 2023. **Revised:** January 8, 2024. **Editorial Decision:** January 15, 2024. **Accepted:** January 15, 2024

Introduction

SOFT syndrome (MIM#614813) denoting Short stature, Onychodysplasia, Facial dysmorphism, and hypoTrichosis, is a rare primordial dwarfism syndrome caused by biallelic *POC1A* variants and encompassing severe growth failure of prenatal onset with dysmorphic features.[1-3] Recently, the phenotypic spectrum has been expanded to include insulin resistance (IR) and diabetes,[4-9] although the pathophysiological mechanisms were not precisely established. POC1A is an important component of centrioles, playing roles in the function of centrosomes and ciliary basal bodies.[10,11] Thus, SOFT syndrome can be considered as a monogenic ciliopathy.[3] In this group of diseases, such as Alström or Bardet-Biedl syndromes, or pericentrin-associated diseases, short stature and/or IR are already known as phenotypic features.[12-18] This suggests a possible unifying mechanism linking some forms of centrosome/cilium dysfunction to growth and metabolic alterations. We present here clinical, genetic, and metabolic characteristics of 2 unrelated patients carrying biallelic *POC1A* null variants. Insulin resistance was associated with central fat distribution, glucose tolerance abnormalities, hypertriglyceridemia, and liver steatosis. Functional studies performed in patients' fibroblasts and in human adipose stem cells (hASCs) with CRISPR/Cas-9 mediated deletion of *POC1A* showed that POC1A protein deficiency impairs ciliogenesis and adipocyte differentiation, induces cellular senescence, and leads to resistance to insulin and IGF1. An altered subcellular localization of insulin receptors, and, to a lesser extent, of IGF1 receptors, could also contribute to resistance to insulin and IGF1.

Methods

Patients

We studied 2 patients from 2 unrelated families, who presented with growth retardation and clinical features suggestive of SOFT syndrome. After written consent, clinical data and blood samples were collected for genotype/phenotype analyses and skin biopsies were performed in the 2 index cases. Consent was obtained from patients and their parents to publish images in Figure 1. The study was approved by the Hospices Civils de Lyon and conducted according to the Declaration of Helsinki principles.

Identification of *POC1A* variants

POC1A variants were identified in patient 1 and patient 2 after sequencing of a next-generation panel and confirmed by Sanger sequencing also performed in patient 1's mother and patient 2's parents. An Array-CGH was performed in patient 2 to narrow the identified deletion.

Clinical, biological, and imagery investigations

Clinical data were obtained during routine follow-up. Endocrinological tests were performed before and during treatment with recombinant human growth hormone (rhGH). Metabolic investigations included measurements of fasting plasma glucose, insulin, glycated hemoglobin (HbA1C), lipid profile, hepatic transaminases, leptin, and adiponectin. The homeostasis model assessment-estimated IR (HOMA-IR) was calculated as fasting glucose (mM) × insulin (mU/L)/22.5.[19] A 120-min oral glucose tolerance test (OGTT with 1.75 g of glucose/kg, maximum 75 g) was

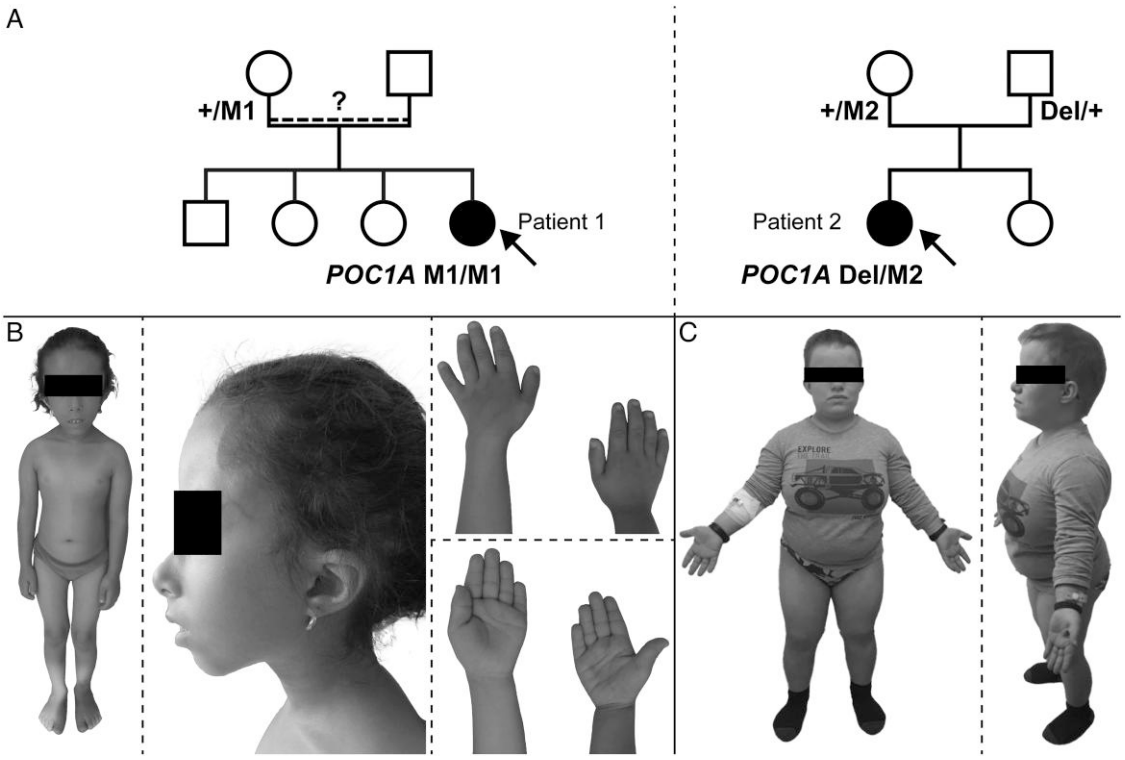

Figure 1. (A) Genealogical trees and familial transmission of the *PO1CA* variants. Arrows indicate probands. Alleles without *POC1A* pathogenic variant, or with *POC1A* deletion, c.145A>T or c.275+2dup variants, are depicted with the symbols +, Del, M1 or M2, respectively. (B) Phenotypic features of patient 1. (C) Phenotypic features of patient 2.

performed with determination of insulin and glucose levels. Body fat percentage and trunk-to-limb fat ratio were measured by dual energy X-rays absorptiometry. Liver fat content and fibrosis were assessed by magnetic resonance imaging (MRI) and elastometry.

Cellular modeling of the disease

Primary fibroblast cultures from patient 1 and patient 2, established after skin biopsy, were compared to commercial control dermal fibroblasts originating from 3 unrelated Caucasian young women (PromoCell, Heidelberg, Germany, #C-12353), used at similar passages. CRISPR/Cas-9 mediated deletion of *POC1A* was performed in hASCs obtained from controls using a previously described method,[20] with a guide RNA (gRNA) targeting *POC1A* exon 3 (sense nucleotide sequence 5′-TCACGCGCCTACCGCTTCAC-3′). Cells transfected with a Cas9/scramble gRNA plasmid were used as controls. Adipocyte differentiation of hASCs was performed as previously described.[21] Cells were studied before exposure to the adipogenic medium and/or after 20 days of differentiation.

Western blot studies

Protein expression studies were performed on whole cell extracts (Table S1 for antibodies). Protein detection and semiquantitative analysis of Western blot vs tubulin were performed using iBright CL1500 imaging system (Invitrogen, Villebon-sur-Yvette, France). The acute maximum effect of insulin or IGF1 on signaling intermediates was assessed on cells maintained in fetal calf serum-free medium for 24 h, then stimulated by 100 nM insulin for 8 min, or 6.5 nM IGF1 for 10 min.

Insulin and IGF1 receptors subcellular localization

The global amount of insulin receptor at the cell membrane was assessed by measuring the ability of cells to bind insulin.[22] Fibroblasts maintained for 16 h in serum-free medium supplemented with 0.1% albumin (Merck, Saint-Quentin-Fallavier, France) were incubated with ^{125}I-insulin (0.3 ng/mL, PerkinElmer, Villebon-sur-Yvette, France), with or without unlabeled insulin (50 nM) in HEPES buffer for 5 h at pH 7.65 and 15 °C. Radioactivity was measured in a gamma counter (PerkinElmer 2470 Wizard2) and results were normalized to the protein content. To evaluate the amount of insulin and IGF1 receptors at the plasma membrane in the vicinity of cilia, we performed co-immunoprecipitation studies using the cilia protein ARL13B as a bait, as described in Supplemental Methods.

Fluorescence and immunofluorescence microscopy studies

Fluorescence and immunofluorescence microscopy studies were performed on cells grown on glass coverslips, then fixed in methanol at −20 °C. DAPI (4,6-di-amidine-2-phenylindole dihydrochloride) was used for nuclear staining. For cilia analysis, cells reaching 80%-90% confluence were cultured in serum-free media for another 48 h to induce ciliogenesis.[23] Centrioles and cilia were stained by antibodies directed against gamma-tubulin and ARL13B, respectively (Table S1). The capacity of adipocytes to store lipids was evaluated by quantification of Oil Red-O staining and lipid-bound, as previously described.[21] Cell proliferation was assessed by measuring bromodeoxyuridine (BrdU) cellular incorporation, and senescence-associated β-galactosidase activity by quantifying the staining of cells after exposure to X-gal (5-bromo-4-chloro-3-indolyl-β-D-galactopyranoside) as previously described.[24] Images were acquired using Olympus IX83 and Olympus FV3000 confocal microscope, and cellSens software (Evident, Rungis, France).

Statistical analyses

Data, all from a minimum of 3 independent experiments, were expressed as means ± SD using the GraphPad Prism 8 software. Statistical significance was evaluated using parametric or nonparametric ANOVA *t*-tests, or Fisher's exact test as required, with a threshold at $P < .05$.

Results

Clinical presentation of patients and identification of biallelic *POC1A* variants

Clinical, biological, and morphological features of the 2 patients are summarized in Table 1.

Patient 1 is a 9.75-year-old French girl born prematurely from healthy parents originating from the same village of Morocco (Figure 1A). Her birth weight and size were extremely low, with a relative macrocephaly. The antenatal karyotype performed for severe intrauterine growth restriction was normal. At 3.75 years old, she was referred to our department for severe growth failure. Her height, weight, and head circumference were respectively 75 cm (−5.5 SDS), 7925 g (−5 SDS), and 46 cm (−1.5 SDS). Her psychomotor development was normal, except for mild language difficulties. She has a high-pitched voice and presents with prominent forehead, triangular face, pointed chin, brief scattered hair at the upper part of the head, short limbs and fingers, and onychodysplasia. Her body fat is predominantly distributed in central areas, with a relative limb lipoatrophy (Figure 1B). Blood tests, endocrinological investigations, and karyotype were normal, except for elevated IGF1 level (+2 SDS). X-rays show short and slender long bones, tall vertebral bodies, and brachydactyly. Treatment with rhGH resulted in a limited increase of height (−5.5 to −4.5 SDS after 4.75 years of rhGH therapy), but was discontinued due to deterioration of glucose tolerance with diabetes diagnosed at OGTT. A GnRH analog was administered from 7.75 to 9.75 years old for central precocious puberty with normal hypothalamo-pituitary MRI.

Next-generation sequencing of a panel dedicated to primordial dwarfism was performed and led to the identification of a homozygous *POC1A* variant ([NM_015426.4]:c.145A>T) that was confirmed by Sanger sequencing. This variant, absent from public databases (ExAC/gnomAD-EVS-GME), predicted to lead to the synthesis of a p.(Lys49*) truncated protein and was classified as pathogenic according to the joint American College of Medical Genetics guidelines (ACMG).[25] Patient's 1 mother was heterozygous for the variant (father not tested).

Patient 2 is a 22-year-old French woman born prematurely from healthy unrelated French parents (Figure 1A). She had extremely low birth weight and size with a relative macrocephaly. During infancy, she was referred to a pediatric endocrinology department for postnatal growth retardation. Blood tests, including endocrinological investigations and karyotype were normal, except IGF1 level (+2 SDS). X-rays showed short and slender long bones, tall vertebral bodies, and brachydactyly. Patient 2 was treated with rhGH therapy from 5 to 8.5 years of age without benefit despite very large doses. At the age of 19, her final height, weight, and head circumference

Table 1. Clinical, biological, and morphological features of the patients.

Features	Patient 1	Patient 2
Development		
Gender	Female	Female
Age at investigation (years)	9.75	19
Origin of parents	Same village of Morocco	French, unrelated
Gestational age at birth	33 SA	33 SA + 3 days
Birth weight (grams)	1090 (−2.2 SDS)	1060 (−2.3 SDS)
Birth length (cm)	35 (−4 SDS)	35 (−4 SDS)
Birth head circumference (cm)	28.5 (−1.5 SDS)	29.5 (−0.5 SDS)
Psychomotor development	Normal	Normal with mild language difficulties
Linear growth	Severe growth failure	Severe growth failure
SOFT syndrome features		
Short stature	Present	Present
Onychodysplasia	Present	Present
Facial dysmorphism	Present	Present
Hypotrichosis	Present	Present
Growth		
Current height (cm)	111 cm (−4.5 SDS)	103.5 cm (−8.5 SDS)
Serum IGF-I level before treatment (µg/L)	245 (+2 SDS)	193 (+2 SDS)
GH peak during stimulation test (µg/L)	24.2	Normal
Bone radiographs	Short and slender long bones, tall vertebral bodies, and brachydactyly	Short and slender long bones, tall vertebral bodies, and brachydactyly
rhGH therapy: ages at onset and discontinuation (years)	5-9.75	5-8.5
Reason for stopping rhGH	Hyperglycemia	Ineffective
Maximum dose of rhGH	35 µg/kg/d	100 µg/kg/d
SDS of height before/after treatment	−5.5 SDS/−4.5 SDS	−8.5 SDS/−8.5 SDS
Maximum serum level of IGF-I under rhGH therapy	697 (>+2 SDS)	NA
Metabolic features		
BMI (kg/m^2)	18.67 (IOTF-25)	27.35
Central distribution of fat	Present	Present
Fasting blood glucose (mmol/L)	4.5	5.1
Fasting insulin (mUI/L)	90	21
HOMA-IR score	18	4.76
HbA1C	5.7%	5.5%
OGTT		
Glycemia at T120min post-OGTT (mmol/L)	11.1	8.4
Insulinemia peak during 2h-OGTT (mUI/L)	1818	263
Hepatic transaminases (AST and ALT)	3N	2.5N
Blood lipid profile (mmol/L)	TG: 1.14—LDL-chol: 2.2—HDL-chol: 1.21	TG: 3.02—LDL-chol: 2.53—HDL-chol: 1.11
Serum leptin (ng/mL)	21.5 (N: 2.69-8.5)	40.76 (N: 7.87-43.5)
Serum adiponectin (µg/mL)	1.76 (N: 3.05-15.6)	2.15 (N: 0.86-21.42)
Dual energy X-rays absorptiometry (DEXA)		
Body fat percentage	48.9%	50.2%
Trunk-to-limb fat ratio	0.93	1.32
Assessment of liver fat content and fibrosis		
Elastography: CAP (dB/m)/E (kPa)	NA	321/5.1
MRI		

(*continued*)

Table 1. Continued

Features	Patient 1	Patient 2
Percentage of liver fat determined by the 2-point Dixon method	8.1%	16.3%
Hepatic steatosis score: percentage of cells with intracellular vacuoles of fat	16%-24% → grade 1 hepatic steatosis	33%-49% → grade 2 hepatic steatosis
Additional characteristics of SOFT syndrome		
Muscle cramps	Absent	Present
High-pitched voice	Present	Present
Empty sella turcica	Absent	NA
Vermian and cerebellar hypotrophy	Present	NA

Abbreviations: CAP, controlled attenuation parameter; E, elastometry; N, normal; NA, not available; IORF, International Obesity Task Force; SDS, standard deviation score.

were respectively 103.5 cm (−8.5 SDS), 29.3 kg (−7 SDS), and 49 cm (−3.5 SDS). She has a high-pitched voice, and presented with prominent forehead, narrow palpebral slits, small extremities, hypotrichosis, and dystrophic nails. Her BMI is 27.35 kg/m^2 and she presents a truncal distribution of fat with a relative paucity of fat in the lower limbs (Figure 1C).

Next-generation sequencing of a panel dedicated to constitutional bone disease was performed at the age of 17 and led to the identification of a *POC1A* heterozygous deletion spanning all exons, and a novel heterozygous intronic splice variant ([NM_015426.4]:c.275+2dup), predicted to lead to the synthesis of a p. (Lys93Leufs*6) truncated protein. The latter, confirmed by Sanger sequencing and absent from genomic databases (ExAC/gnomAD-EVS-GME) was classified as likely pathogenic.[25] Array-CGH confirmed the presence of a 102.6 kb heterozygous deletion at 3p21.2 involving only *POC1A* (3p21.2(521 1 51 18_522177 35)×1) (hg19). Genotyping of parents identified the intronic variant in her mother and the deletion in her father.

Figure 2 shows a schematic representation of *POC1A* gene and protein with the pathogenic variants newly identified or previously reported.[1-9,26-33]

Endocrinological and metabolic explorations reveal clinical, biological, and morphological signs related to resistance to IGF1 and insulin

Elevated plasma IGF1 levels, before and during rhGH therapy, and normal or excessive GH response during stimulation tests, suggested that patient 1 and patient 2 present a state of resistance to IGF1 (Table 1).

Both patients were overweight, with a high percentage of body fat (48.9% and 50.2%, respectively), in line with leptin levels (Table 1). Clinically, excess fat mass predominated at the truncal level in both patients. The 2 patients presented with biological signs of IR with fasting hyperinsulinemia, which reached 90 mU/L in patient 1, with normal fasting glucose. Oral glucose tolerance test revealed diabetes (patient 1) or impaired glucose tolerance (patient 2) and major post-stimulated hyperinsulinemia. Both patients had elevated liver enzymes related to hepatic steatosis. Patient 2 had hypertriglyceridemia, and patient 1 decreased adiponectin levels. Taken together, these data show that patients with biallelic *POC1A* variants presented with severe IR.

Cellular modeling

POC1A variants identified in patients 1 and 2 result in the loss of POC1A protein expression and in altered centrosome/basal body organization and ciliogenesis in fibroblasts

Pathogenic variants in *POC1A* found in patient 1 (in a homozygous state) and in patient 2 (in a hemizygous state) are predicted to disrupt the amino acid sequence of the protein in its N-terminal region, close to its third WD40-repeat domain (Figure 2). The protein expression of POC1A is not detectable in patients' fibroblasts (Figure 3A). Given the well-established role of POC1A in ciliogenesis,[11] we investigated the consequences of *POC1A* deficiency on the organization of cilia and centrosome/basal bodies in patients' cells. We found that fibroblasts from patients exhibit a higher frequency of abnormal, curved-shaped cilia, or are even devoid of cilia compared to control fibroblasts, as assessed by immunofluorescence studies (Figure 3B). Fragmentation and/or multiplication of

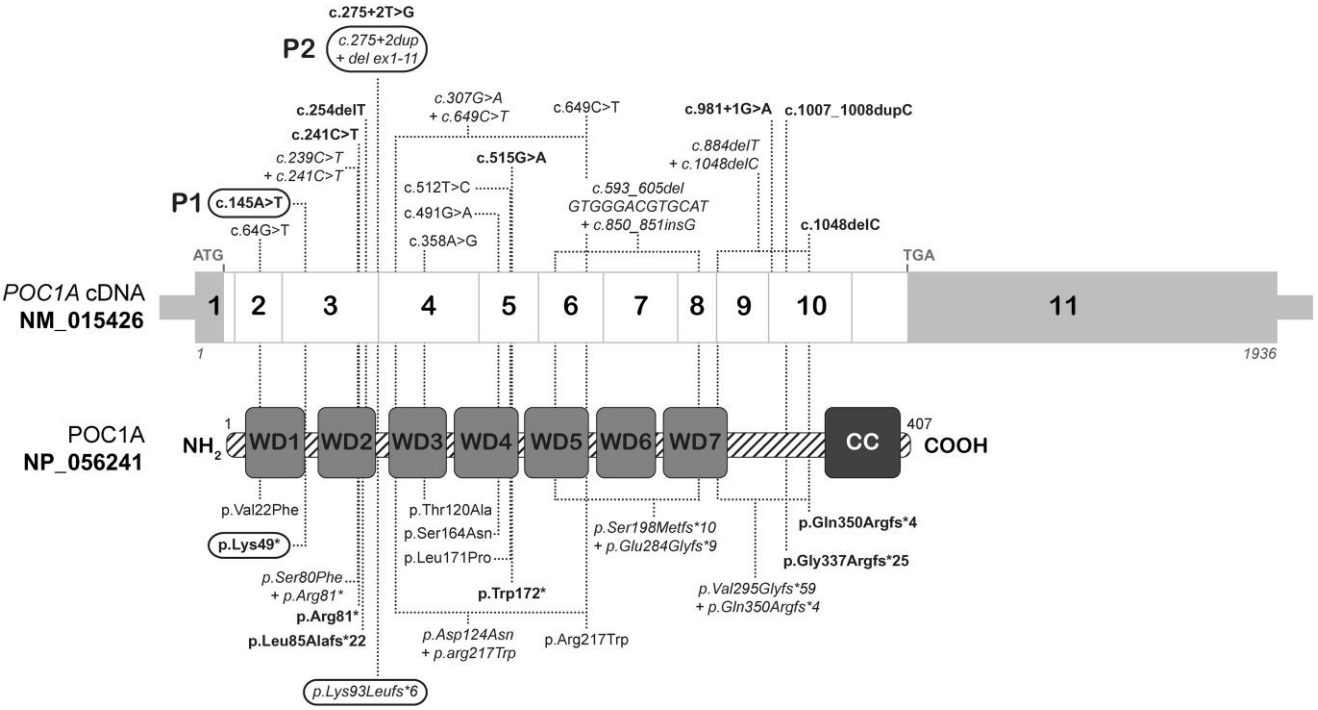

Figure 2. Schematic representation of *POC1A* gene and protein (long isoform). The predicted localization of previously reported,[1-9,25-32] and newly identified *POC1A* pathogenic variants (boxed) is depicted within cDNA and protein sequences. Corresponding accession numbers, and coding (white boxes) and noncoding (gray boxes) *POC1A* exons are indicated. N-terminal 7 β-propeller WD40 and C-terminal coiled-coil functional domains are depicted. Homozygous *POC1A* variants are indicated, in bold font for frameshift, truncating or intronic splice variants. Compound heterozygous *POC1A* variants are depicted in italics.

centrosomes/basal bodies are more frequent in patients' fibroblasts than in control cells (Figure 3C).

Fibroblasts from patients with biallelic *POC1A* null variants show impaired insulin and IGF1 signaling

Since patients 1 and 2 display signs of IR (elevated insulin and glucose serum levels) and IGF1 resistance (increased IGF1 and GH serum levels), we investigated the insulin- and IGF1-mediated activation of proximal signaling intermediates in cultured fibroblasts. We found that ligand-mediated activation of the receptors and metabolic and mitogenic intermediates of insulin and IGF1 pathways (ie, IRS1, AKT, and ERK1/2) were significantly impaired in fibroblasts from patients with *POC1A* null variants compared to control cells (Figure 4A). Importantly, the total amount of insulin and IGF1 receptors in whole protein extracts from patients' cells did not show any significant decrease. Given that cilia have been shown to recruit insulin and IGF1 receptors to the plasma membrane and regulate signaling events,[15,34-37] a hypothesis could be that impaired ciliogenesis result in abnormal subcellular localization of insulin and/or IGF1 receptors. To test this hypothesis, we performed co-immunoprecipitation studies using the cilia protein ARL13B as a bait. The amount of insulin receptors, and to a lesser extent of IGF1 receptors co-immunoprecipitated with ARL13B, was reduced in patients' cells compared to controls (Figure 4B). Additionally, we assessed the ability of fibroblasts from patient 1 to bind insulin and observed a ~30% decrease compared to control cells (Figure 4C). Taken together, these results suggest that the amount of insulin receptor at the cell membrane could be decreased in fibroblasts carrying *POC1A* null variants.

Fibroblasts from patients with biallelic *POC1A* null variants show impaired proliferation capacity and increased senescence markers

Dysfunction of cilia is associated with accelerated tissue and cellular aging,[38] which could participate to growth retardation, alterations in adipose tissue, and resistance to insulin and/or IGF1. Therefore, we investigated whether the *POC1A* null variants identified in the patients could impair cell replicative capacity and/or induce cellular senescence. Cellular proliferation, assessed by the capacity of BrdU incorporation, was significantly reduced in patients' fibroblasts compared to control cells (Figure 5A). In addition, senescence-activated-β-galactosidase activity and the protein expression of the cell cycle arrest markers, including phospho-p53, p16 and p21, were significantly increased in patients' fibroblasts compared to controls (Figure 5B and C).

Deletion of *POC1A* in hASCs recapitulated altered ciliogenesis, resistance of insulin and IGF1, impaired proliferation and increased senescence, and lead to adipocyte differentiation defects

Patients 1 and 2 with *POC1A* null variants are characterized by IR associated with a central repartition of fat with relative limb lipoatrophy. To evaluate whether adipocyte differentiation defects in *POC1A*-deleted cells could lead to the metabolic phenotype of the disease, we conducted a CRISPR/Cas-9-mediated deletion of *POC1A* in hASCs. We observed that POC1A deficiency in undifferentiated hASCs recapitulated the cellular phenotype observed in patients' fibroblasts, including defects in cellular organization of centrosome/basal bodies and cilia, impaired insulin and IGF1 signaling, and increased cellular senescence (Figure 6), indicating that adipocyte precursors play a

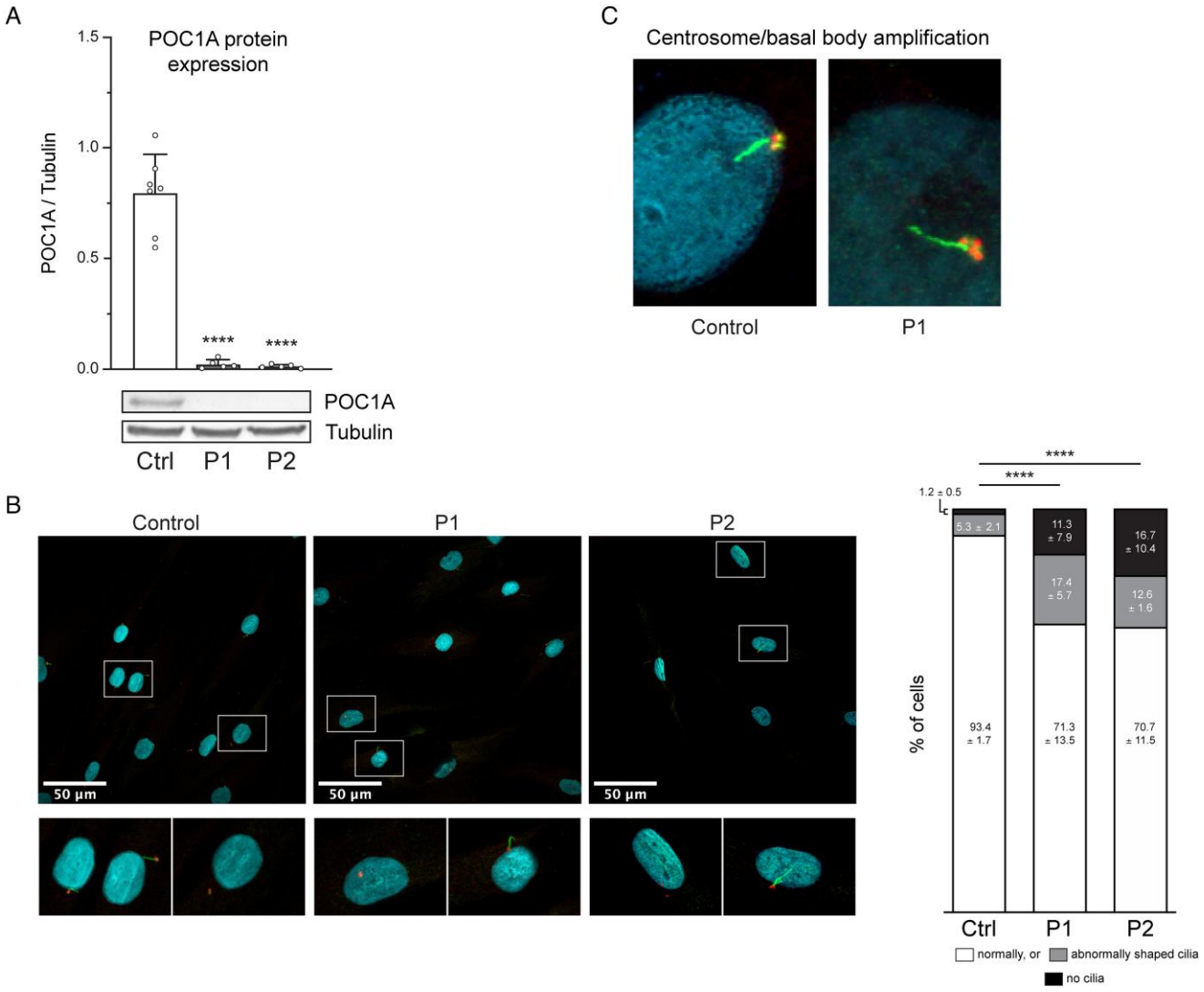

Figure 3. Fibroblasts from patients harboring biallelic *POC1A* pathogenic variants show a lack of POC1A protein expression and defects in cilia and basal body organization. (A) Protein expression of POC1A assessed by Western blotting in fibroblasts from controls and patients. Representative images of Western blots (5 independent experiments), and quantitative measurements (means ± SD) are shown. Tubulin is used as an index of the cellular protein level. ****$P < .0001$ vs control. Immunocytological features of cilia (B) and centrosome/basal body organization (C) in fibroblasts from controls and patients. Cell nuclei are stained in blue with DAPI. Centrioles are revealed by red anti-γ-tubulin staining, and cilia by green anti-ARL13B staining. Scale bar: 50 µm. Representative photographs are shown, with magnification of cells depicted by rectangles. The percentage of cells with normal cilia (white boxes), abnormally shaped cilia (gray boxes), and of cells without cilia (black boxes) was evaluated on a total number of 979 control and 1114 patients' cells and expressed as means ± SD. ****$P < .0001$ vs control. Fragmentation and/or multiplication of centrosomes/basal bodies was observed in 16% of patients' cells vs 2% of control cells (observation of 50 cells of each condition).

role in the disease. Furthermore, the deletion of *POC1A* strikingly impaired adipocyte differentiation, as shown by the absence of lipid storage of *POC1A* knockout hASCs exposed to an adipogenic medium, as compared to control cells (Figure 7A and B). In line, the protein expression of key adipogenic factors such as CCAAT/enhancer binding protein alpha (C/EBPα), sterol regulatory element-binding protein 1c (SREBP1c) and peroxisome proliferator-activated receptor gamma (PPARγ), as well as the mature adipocyte proteins perilipin-1, fatty acid synthase, leptin, and adiponectin, were significantly reduced in *POC1A*-deleted hASCs compared to control cells during *in vitro* adipocyte differentiation (Figure 7C).

Discussion

This translational study confirms that severe IR can be a prominent feature of SOFT syndrome linked to biallelic *POC1A* null variants. It also demonstrates that patients can additionally present with resistance to IGF1. This study shows that the disease is associated with central fat distribution, glucose tolerance abnormalities, hypertriglyceridemia and liver steatosis, and impaired *in vitro* adipocyte differentiation, suggesting that adipose tissue dysfunction could primarily lead to the metabolic phenotype. In addition, abnormal cilia and centrosome/basal body organization within cells could induce cell-autonomous signaling defects due to accelerated senescence, and impaired subcellular localization of insulin receptors, and to a lesser extent, IGF1 receptors at the plasma membrane, which may contribute to metabolic alterations. Given that other monogenic ciliopathies also show adipose tissue involvement and IR, it is tempting to speculate that a unifying mechanism arising from altered ciliogenesis might underlie the metabolic features associated with Bardet-Biedl, Alström, *PCNT*-related lipodystrophy, and SOFT syndrome.

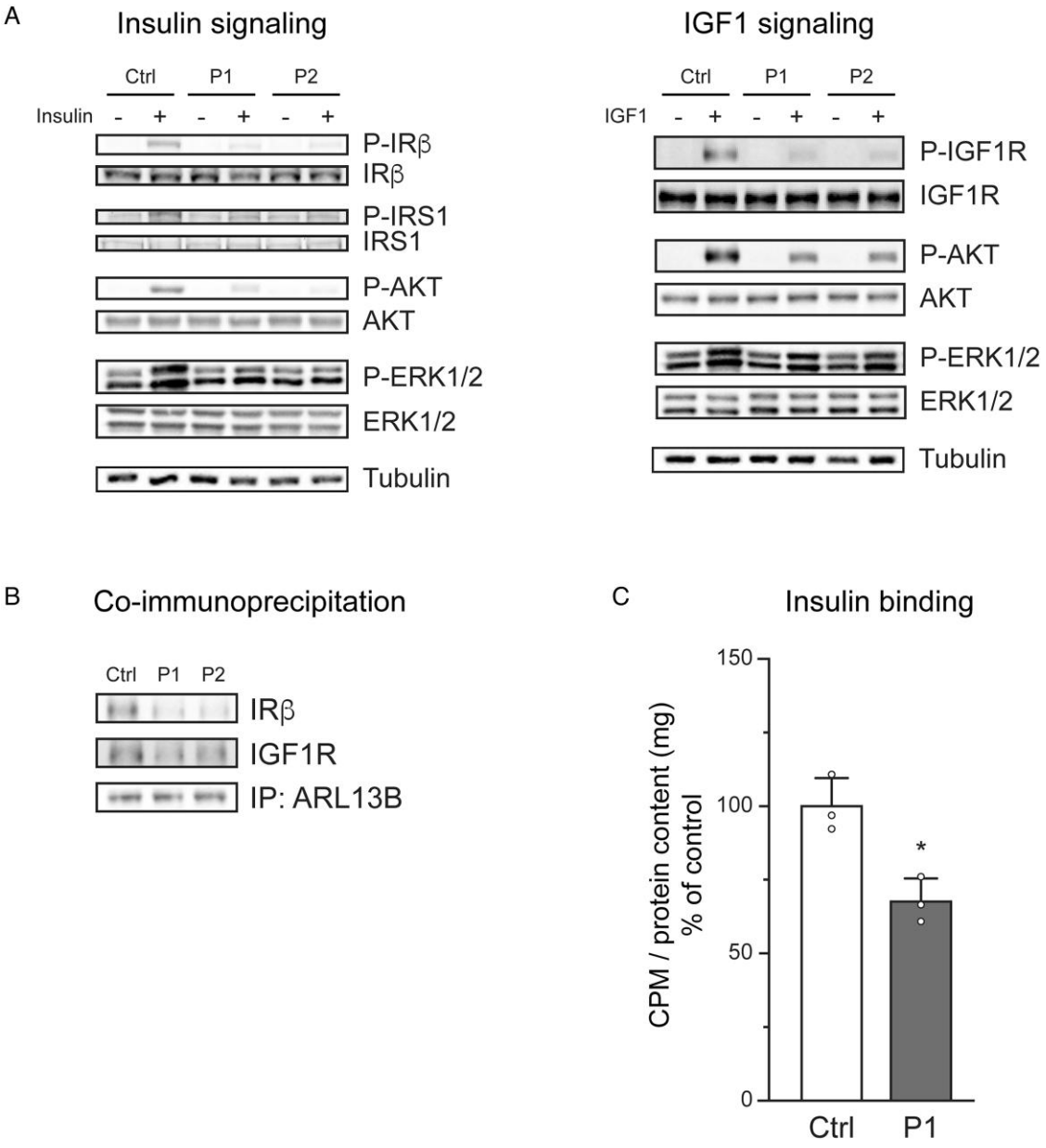

Figure 4. Fibroblasts from patients with *POC1A* null variants are resistant to the effects of insulin and IGF1. (A) Insulin- and IGF1-induced activation of signaling intermediates was evaluated by Western blotting in fibroblasts from controls and patients. The total protein expression of the signaling intermediates insulin receptor β-subunit (IRβ), IGF1 receptor (IGF1-R), insulin receptor substrate-1 (IRS1), protein kinase B (AKT) and extracellular-regulated kinase (ERK) 1/2, and of their insulin or IGF1-activated forms (P-: phosphorylated proteins) were evaluated using antibodies listed in Table S1. Insulin-mediated phosphorylation of IRβ and IRS1 were assessed using antibodies directed against phospho-tyrosine residues. Tubulin is an index of the cellular protein level. Blots are representative of 3 or 4 independent experiments. Western blot quantifications are available in Figure S1A. (B) Co-immunoprecipitation studies using the cilia protein ARL13B as a bait. The amount of insulin and IGF1 receptors co-immunoprecipitated with ARL13B was evaluated by Western blotting in fibroblasts from controls and patients. See Table S1 for details regarding antibodies, and Figure S1B for Western blot quantifications. (C) The ability of fibroblasts from patient 1 to bind insulin to its receptor was evaluated using ^{125}I-insulin (counts per minute [CPM] normalized to protein content). Results from 3 independent experiments are expressed as the percentage of insulin binding as compared to controls (means ± SD). *$P < .05$ vs control.

The phenotype of severe IR associated with SOFT syndrome was initially described in patients with frameshift *POC1A* variants affecting exon 10 of the gene.[4-6] *POC1A* exon 10 is naturally skipped in one of the *POC1A* mRNA transcripts, and is retained in other transcripts. It was thus hypothesized that specific *POC1A* variants, which could lead to the production of transcripts lacking exon 10, may cause a "variant POC1A-related syndrome" (vPOC1A) characterized by typical features of SOFT syndrome associated with IR.[4,5] However, metabolic investigations were lacking in several studies, and subsequent reports pointed out that IR could be present in patients carrying *POC1A* biallelic variants regardless of their position.[7-9] SOFT syndrome-associated IR was shown to develop progressively from childhood to adulthood,[6] which is confirmed in the current study. Progression from IR to diabetes is a significant risk, which could be favored by rhGH therapy as highlighted in previous reports and in our observations.[1,3,7,8,18,39,40] However, to our knowledge, diabetes related to SOFT syndrome has not been diagnosed in patients as young as patient 1 from our study. This should encourage clinicians to regularly perform OGTT in

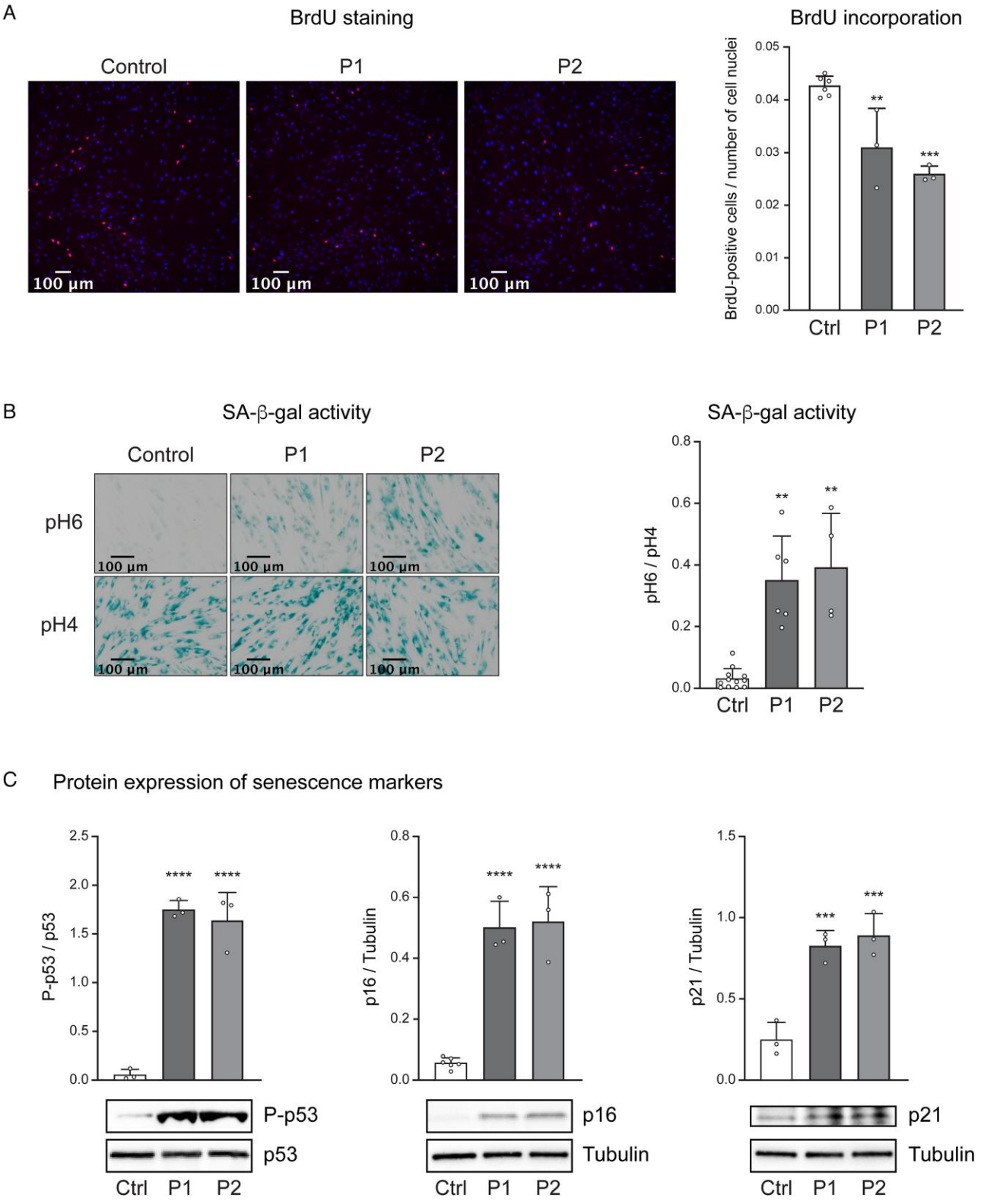

Figure 5. Fibroblasts from patients with biallelic *POC1A* null variants show impaired proliferation capacity and increased senescence markers. (A) Cellular proliferation was assessed by the capacity of fibroblasts to incorporate BrdU. Cell nuclei stained by anti-BrdU antibodies were identified by immunofluorescence microscopy (red staining) and counted relative to total nuclei (blue DAPI staining). Results (means ± SD) are from 3 independent experiments. Scale bar: 100 µm. $^{**}P < .01$, $^{***}P < .001$ vs control. (B) Senescence-activated-β-galactosidase activity of cells was assessed by the ratio of X-gal staining at pH6 to nonspecific staining at pH4. Representative images and quantitative measurements from 4 independent experiments are shown (means ± SD). Scale bar: 100 µm. $^{**}P < .01$ vs control. (C) The protein expression of the cell cycle arrest markers phospho-p53 (P-p53) as compared to total p53, and p16 and p21 normalized to tubulin, was evaluated by Western blotting in fibroblasts from controls and patients. Representative blots (from 3 independent experiments) and quantitative measurements (means ± SD) are shown. $^{***}P < .001$, $^{****}P < .0001$ vs control.

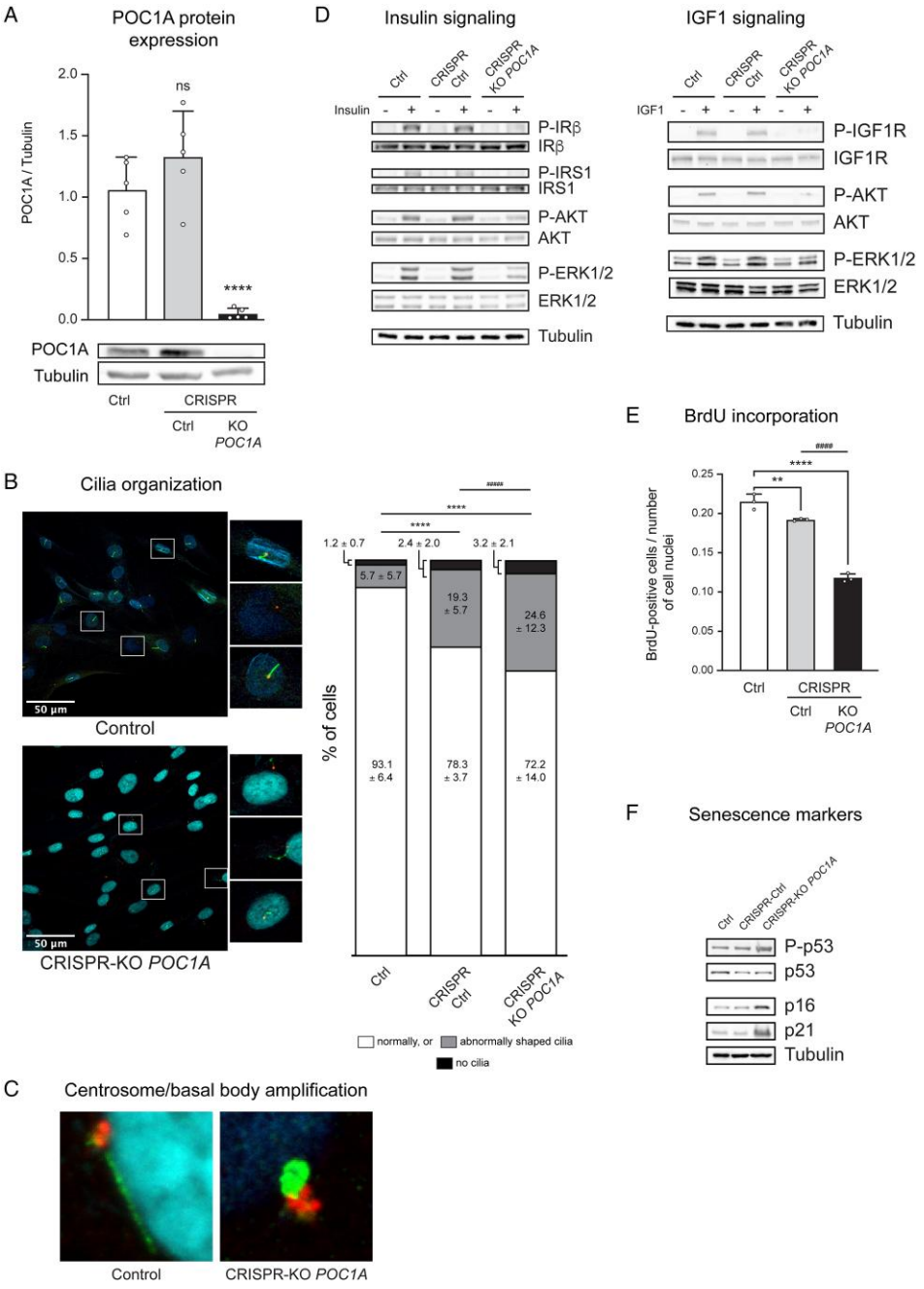

Figure 6. CRISPR-Cas9-mediated deletion of *POC1A* in hASCs recapitulates altered ciliogenesis, resistance to insulin and IGF1, impaired proliferation and increased senescence. Data were obtained in control hASCs (Ctrl), hASCs transfected with a Cas9/scramble gRNA plasmid (CRISPR-Ctrl), or hASCs submitted to a CRISPR-Cas9-mediated *POC1A*-knockout (CRISPR-KO *POC1A*), cultured in a maintenance medium (non-differentiated hASCs). Experiments were conducted as described in fibroblasts. (A) Validation of the CRISPR-Cas9-mediated deletion of *POC1A* in hASCs. Representative images of Western blots performed in triplicate, and quantitative measurements (means ± SD) are shown. Tubulin is used as an index of the cellular protein level. $^{****}P < .0001$ vs Ctrl, ns: not significant. Immunocytological features of cilia (B) and centrosome/basal body organization (C) in hASCs. Cell nuclei are stained in blue with DAPI. Centrioles are revealed by red anti-γ-tubulin staining, and cilia by green anti-ARL13B staining. Scale bar: 50 µm. Representative photographs are shown, with magnification of cells depicted by rectangles. The percentage of cells with normal cilia (white boxes), abnormally shaped cilia (gray boxes), and of cells without cilia (black boxes) was evaluated on a total number of 310 control hASCs, 371 CRISPR-Ctrl, and 1045 CRISPR-KO *POC1A* hASCs and expressed as means ± SD. $^{****}P < .0001$ vs Ctrl hASCs, $^{\#\#\#\#}P < .0001$ vs CRISPR-Ctrl hASCs. We observed fragmentation and/or multiplication of centrosomes/basal bodies in several CRISPR-KO *POC1A* hASCs (29% of the cells), but in rare control hASCs (less than 2%) (observation of 40 cells of each condition). (D) Insulin- and IGF1-induced activation of signaling intermediates in hASCs. The total protein expression of the signaling intermediates insulin receptor β-subunit (IRβ), IGF1 receptor (IGF1-R), insulin receptor substrate-1 (IRS1), protein kinase B (AKT) and extracellular-regulated kinase (ERK)1/2, and of their insulin or IGF1-activated forms (P-: phosphorylated proteins) were evaluated using antibodies listed in Table S1. Insulin-mediated phosphorylation of IRβ and IRS1 was assessed using antibodies directed against phospho-tyrosine residues. Tubulin is an index of the cellular protein level. Blots are representative of 3 independent experiments. Western blot quantifications are available in Figure S2A. (E) Cell proliferation in hASCs. Cellular proliferation was assessed by measuring the ratio of cells positive for anti-BrdU staining to total nuclei stained by DAPI. Results (means ± SD) are from 3 independent experiments. $^{**}P < .01$, $^{****}P < .0001$ vs Ctrl hASCs, $^{\#\#\#\#}P < .0001$ vs CRISPR-Ctrl hASCs. (F) Protein expression of senescence markers in hASCs. The protein expression of the senescence markers phospho-p53 (P-p53) as compared to total p53, and p16 and p21 as compared to tubulin was assessed by Western blotting. Representative blots (from 3 independent experiments) are shown. Western blot quantifications are available in Figure S2B.

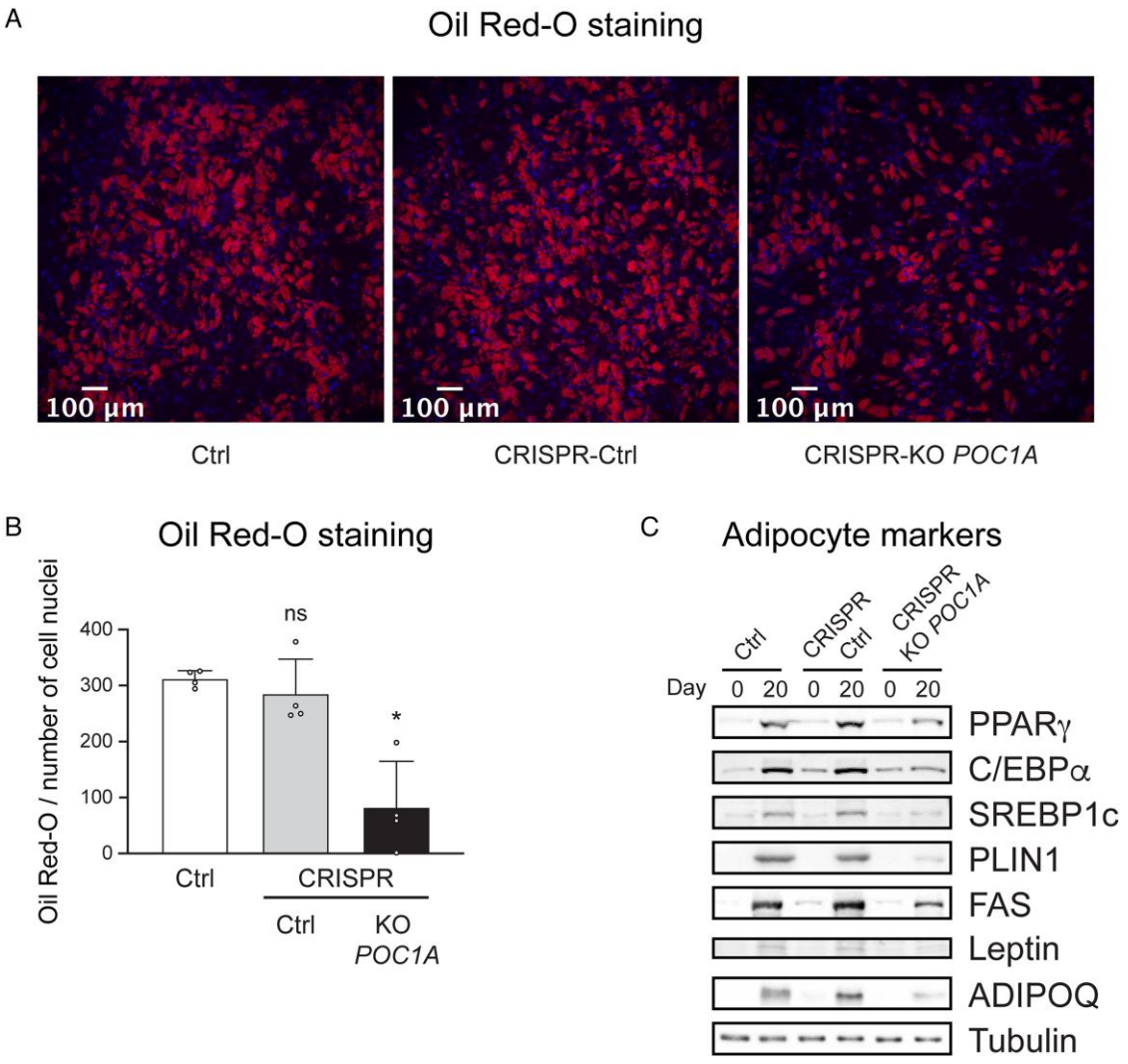

Figure 7. CRISPR-Cas9-mediated deletion of *POC1A* impairs adipocyte differentiation of human adipose stem cells. Data were obtained in control hASCs (Ctrl), hASCs transfected with a Cas9/scramble gRNA plasmid (CRISPR-Ctrl), or hASCs submitted to a CRISPR-Cas9-mediated *POC1A*-knockout (CRISPR-KO *POC1A*), cultured in a maintenance medium (non-differentiated cells, day 0) or in an adipogenic medium for 20 days as indicated (day 20). (A) Oil Red-O red staining of intracellular lipids was evaluated at day 20 of adipocyte differentiation by fluorescence microscopy. Cell nuclei are stained in blue by DAPI. Representative images are shown. (B) Quantification of Oil Red-O fluorescence was normalized to DAPI staining and expressed as means ± SD of 4 independent experiments. $*P < .05$ vs Ctrl hASCs, ns: not significant. (C) Protein expression of adipogenic factors and mature adipocyte markers as assessed by Western blotting in hASCs studied at day 0 and day 20 of adipocyte differentiation. C/EBPα, CCAAT/enhancer binding protein alpha; SREBP1c, sterol regulatory element-binding protein 1c; PPARγ, peroxisome proliferator-activated receptor gamma; PLIN1, perilipin-1; FAS, fatty acid synthase; ADIPOQ, adiponectin. Tubulin is used as a loading control. Images are representative of 3 independent experiments. See Figure S2C for Western blot quantifications.

patients with SOFT syndrome, even before puberty, to detect IR and/or glucose tolerance abnormalities as soon as possible. Measures promoting healthy diet and physical activity should be given to patients and their families from an early age. Our observation, in conjunction with previous reports, suggests that *POC1A* should be considered as a gene involved in monogenic IR, lipodystrophy and/or diabetes.[8]

Our study shed new light on the pathophysiological mechanisms of IR in SOFT syndrome. Since POC1A is an important luminal component of centrioles, playing roles in the function of centrosomes, spindle poles, and ciliary basal bodies, SOFT syndrome could be considered as a monogenic cause of ciliopathy.[3,10,11] Other genetic defects responsible for ciliopathy most notably Alström and Bardet-Biedl syndromes, are associated with obesity and IR.[12,13,16] Although it is unclear whether IR is disproportionate to the degree of obesity in Bardet-Biedl syndrome, adipose tissue dysfunction could play a specific role in the pathophysiology of IR associated with Alström syndrome.[13] In Bardet-Biedl syndrome, defects in the BBSome complex impair the neuronal cilia-mediated trafficking, resulting in abnormal cellular localization of proteins involved in the regulation of satiety.[41,42] Although most forms of primordial dwarfism have not been associated with severe IR, it is described in *PCNT*-related lipodystrophy due to abnormalities in the centrosomal protein pericentrin.[17,18] Thus, it appears that a subset of genetic defects affecting the centrosome gives rise to IR, suggesting that dysregulated function of certain centriolar and pericentriolar proteins is linked to defective adipose tissue maintenance, regeneration and/or response to insulin. Our study reveals that POC1A deficiency induces defects in adipose differentiation of hASCs, which suggests that adipocyte dysfunction drives, at least in part, the metabolic alterations associated with

the disease. These results, and the clinical phenotype of the disease, which comprises a relative limb lipoatrophy contrasting with increased abdominal fat, with glucose tolerance abnormalities and hyperinsulinemia, dyslipidemia, and liver steatosis, suggest that SOFT syndrome could be considered as a lipodystrophic syndrome. Interestingly, adipocyte differentiation defects have been previously identified in Alström syndrome,[13] and in *PCNT*-associated diseases.[18] Our results also show that POC1A deficiency is associated with decreased cell proliferation and accelerated cell senescence in human fibroblasts and adipose stem cells, and may induce a mislocalization of insulin and IGF1 receptors at the plasma membrane in fibroblasts. These different cellular features could be mechanistically linked, since cilia dynamics and protein recruitment have been shown to regulate cell aging,[38] and adipogenesis,[36,43] the latter also depending on the recruitment of IGF1-R at the vicinity of the primary cilium.[34,35] To note, Bardet-Biedl syndromes proteins were also shown to regulate insulin receptor trafficking.[15,37]

Concerning the short stature associated with SOFT syndrome, the underlying mechanisms could be multiple. Defects of chondrocyte proliferation and survival in the growth plate of long bones have been observed in animal models with *POC1A* defects. Multipolar spindle formation due to defective ciliary function in chondrocytes could result in their inability to proliferate and to maintain the flattened shape required to form a cellular column after cell division.[26,44] Our study suggests that a state of resistance to IGF1 could also contribute to growth retardation. An elevated serum IGF-1 level (>+2 SDS) was reported in 2 of the 3 patients evaluated in previous studies, in favor of this hypothesis.[7,9] Although further studies in humans are required to elucidate the function of *POC1A* in endochondral ossification and growth, both defects in chondrocyte proliferation and in response to IGF1 could contribute to the poor response to rhGH therapy, which is reported in SOFT syndrome in several studies including ours.[1,2,26-30] As rhGH therapy could worsen IR and precipitate diabetes, we agree that rhGH treatment is not indicated in SOFT syndrome and should even be avoided.[7]

Our study has several limitations. We studied only 2 patients with biallelic *POC1A* pathogenic variants. However, since both of them showed a complete lack of POC1A expression, this allowed us to use a *POC1A* knockout cell model of the disease. Although our study reveals several mechanisms associated with insulin and IGF1 resistance, we were not able to clearly show whether adipose tissue involvement, or primary defects in insulin signaling, drives the metabolic defects. In favor of the first hypothesis, patients present with liver steatosis and dyslipidemia, and normal-to-decreased adiponectin level, which are signs of lipodystrophy-associated, rather than receptoropathy-associated IR.[45]

Whatever the underlying mechanisms, IR is an important feature in patients with SOFT syndrome, which requires regular clinical and biological metabolic monitoring. We suggest that sequencing of *POC1A* should be performed more broadly in children with short stature, IR and/or centripetal fat distribution.

Acknowledgments

We thank the patients and families who participated in this study. C.V. is member of the European Reference Network on Rare Endocrine Conditions—project ID no. 739527.

Supplementary material

Supplementary material is available at *European Journal of Endocrinology* online.

Funding

This work was supported by institutional fundings from the Institut National de la Santé et de la Recherche Médicale (Inserm), Sorbonne Université, Assistance-Publique Hôpitaux de Paris, Alliance Nationale pour les Sciences de la Vie et de la Santé (Aviesan, ITMO Cancer), Institut National du Cancer (INCa), and the French Ministry of Health and of Higher Education and Research (Plan National Maladies Rares 3), by the Fondation pour la Recherche Médicale (grant number EQU201903007868), and by the Association Française des Lipodystrophies (AFLIP), through a donation to the Association Robert-Debré pour la Recherche Médicale (ARDRM). J.G. is funded by the Fondation pour la Recherche Médicale (EQU202003010517), the Mairie de Paris (Emergences—R18139DD), and the Agence Nationale de la Recherche (ANR-21-CE18-0002-01).

Conflict of interest: None declared.

Authors' contributions

Kevin Perge (Conceptualization [equal], Data curation [equal], Formal analysis [equal], Investigation [equal], Methodology [equal], Resources [equal], Software [equal], Validation [equal], Writing—original draft [equal], Writing—review & editing [equal]), Emilie Capel (Conceptualization [equal], Data curation [equal], Formal analysis [equal], Investigation [equal], Methodology [equal], Resources [equal], Software [equal], Validation [equal], Writing—original draft [equal], Writing—review & editing [equal]), Carine Villanueva (Conceptualization [equal], Data curation [equal], Investigation [equal], Validation [equal], Writing—original draft [equal], Writing—review & editing [equal]), Jérémie Gautheron (Formal analysis [equal], Funding acquisition [equal], Investigation [equal], Methodology [equal], Resources [equal], Writing—review & editing [equal]), Safiatou Diallo (Formal analysis [equal], Investigation [equal], Methodology [equal], Resources [equal], Writing—review & editing [equal]), Martine Auclair (Formal analysis [equal], Investigation [equal], Methodology [equal], Resources [equal], Writing—review & editing [equal]), Sophie Rondeau (Data curation [equal], Formal analysis [equal], Investigation [equal], Writing—review & editing [equal]), Romain Morichon (Data curation [equal], Formal analysis [equal], Investigation [equal], Writing—review & editing [equal]), Frédéric Brioude (Data curation [equal], Formal analysis [equal], Investigation [equal], Writing—review & editing [equal]), Isabelle Jéru (Data curation [equal], Formal analysis [equal], Investigation [equal], Writing—review & editing [equal]), Massimiliamo Rossi (Data curation [equal], Formal analysis [equal], Investigation [equal], Writing—review & editing [equal]), Marc Nicolino (Conceptualization [equal], Data curation [equal], Formal analysis [equal], Investigation [equal], Methodology [equal], Resources [equal], Software [equal], Supervision [equal], Validation [equal], Writing—original draft [equal], Writing—review & editing [equal]), and Corinne Vigouroux (Conceptualization [equal], Data curation [equal], Formal analysis [equal], Funding acquisition [equal], Investigation [equal], Methodology [equal], Resources [equal], Software [equal], Supervision [equal], Validation [equal], Writing—original draft [equal], Writing—review & editing [equal])

Data availability

Data that support the findings of this study are included in this article or available from the corresponding author upon reasonable request.

References

1. Shalev SA, Spiegel R, Borochowitz ZU. A distinctive autosomal recessive syndrome of severe disproportionate short stature with short long bones, brachydactyly, and hypotrichosis in two consanguineous Arab families. *Eur J Med Genet*. 2012;55(4):256-264. https://doi.org/10.1016/j.ejmg.2012.02.011
2. Sarig O, Nahum S, Rapaport D, *et al*. Short stature, onychodysplasia, facial dysmorphism, and hypotrichosis syndrome is caused by a POC1A mutation. *Am J Hum Genet*. 2012;91(2):337-342. https://doi.org/10.1016/j.ajhg.2012.06.003
3. Shaheen R, Faqeih E, Shamseldin HE, *et al*. POC1A truncation mutation causes a ciliopathy in humans characterized by primordial dwarfism. *Am J Hum Genet*. 2012;91(2):330-336. https://doi.org/10.1016/j.ajhg.2012.05.025
4. Chen JH, Segni M, Payne F, *et al*. Truncation of POC1A associated with short stature and extreme insulin resistance. *J Mol Endocrinol*. 2015;55(2):147-158. https://doi.org/10.1530/JME-15-0090
5. Giorgio E, Rubino E, Bruselles A, *et al*. A syndromic extreme insulin resistance caused by biallelic POC1A mutations in exon 10. *Eur J Endocrinol*. 2017;177(5):K21-K27. https://doi.org/10.1530/EJE-17-0431
6. Majore S, Agolini E, Micale L, *et al*. Clinical presentation and molecular characterization of a novel patient with variant POC1A-related syndrome. *Clin Genet*. 2021;99(4):540-546. https://doi.org/10.1111/cge.13911
7. Mericq V, Huang-Doran I, Al-Naqeb D, *et al*. Biallelic POC1A variants cause syndromic severe insulin resistance with muscle cramps. *Eur J Endocrinol*. 2022;186(5):543-552. https://doi.org/10.1530/EJE-21-0609
8. Li D, Li S, Zhou J, *et al*. Case Report: identification of a rare nonsense mutation in the POC1A gene by NGS in a diabetes mellitus patient. *Front Genet*. 2023;14:1113314. https://doi.org/10.3389/fgene.2023.1113314
9. Li G, Chang G, Wang C, *et al*. Identification of SOFT syndrome caused by a pathogenic homozygous splicing variant of POC1A: a case report. *BMC Med Genomics*. 2021;14(1):207. https://doi.org/10.1186/s12920-021-01055-1
10. Pearson CG, Osborn DPS, Giddings TH Jr, Beales PL, Winey M. Basal body stability and ciliogenesis requires the conserved component Poc1. *J Cell Biol*. 2009;187(6):905-920. https://doi.org/10.1083/jcb.200908019
11. Venoux M, Tait X, Hames RS, Straatman KR, Woodland HR, Fry AM. Poc1A and Poc1B act together in human cells to ensure centriole integrity. *J Cell Sci*. 2013;126(1):163-175. https://doi.org/10.1242/jcs.111203
12. Collin GB, Marshall JD, Ikeda A, *et al*. Mutations in ALMS1 cause obesity, type 2 diabetes and neurosensory degeneration in Alström syndrome. *Nat Genet*. 2002;31(1):74-78. https://doi.org/10.1038/ng867
13. Geberhiwot T, Baig S, Obringer C, *et al*. Relative adipose tissue failure in Alström syndrome drives obesity-induced insulin resistance. *Diabetes*. 2021;70(2):364-376. https://doi.org/10.2337/db20-0647
14. Romano S, Maffei P, Bettini V, *et al*. Alström syndrome is associated with short stature and reduced GH reserve. *Clin Endocrinol (Oxf)*. 2013;79(4):529-536. https://doi.org/10.1111/cen.12180
15. Starks RD, Beyer AM, Guo DF, *et al*. Regulation of insulin receptor trafficking by Bardet Biedl syndrome proteins. *PLoS Genet*. 2015;11(6):e1005311. https://doi.org/10.1371/journal.pgen.1005311
16. Jeziorny K, Antosik K, Jakiel P, Młynarski W, Borowiec M, Zmysłowska A. Next-generation sequencing in the diagnosis of patients with Bardet–Biedl syndrome—new variants and relationship with hyperglycemia and insulin resistance. *Genes (Basel)*. 2020;11(11):1283. https://doi.org/10.3390/genes11111283
17. Rauch A, Thiel CT, Schindler D, *et al*. Mutations in the pericentrin (PCNT) gene cause primordial dwarfism. *Science*. 2008;319(5864):816-819. https://doi.org/10.1126/science.1151174
18. Huang-Doran I, Bicknell LS, Finucane FM, *et al*. Genetic defects in human pericentrin are associated with severe insulin resistance and diabetes. *Diabetes*. 2011;60(3):925-935. https://doi.org/10.2337/db10-1334
19. Matthews DR, Hosker JP, Rudenski AS, Naylor BA, Treacher DF, Turner RC. Homeostasis model assessment: insulin resistance and beta-cell function from fasting plasma glucose and insulin concentrations in man. *Diabetologia*. 1985;28(7):412-419. https://doi.org/10.1007/BF00280883
20. Gautheron J, Lima L, Akinci B, *et al*. Loss of thymidine phosphorylase activity disrupts adipocyte differentiation and induces insulin-resistant lipoatrophic diabetes. *BMC Med*. 2022;20(1):95. https://doi.org/10.1186/s12916-022-02296-2
21. Sollier C, Capel E, Aguilhon C, *et al*. LIPE-related lipodystrophic syndrome: clinical features and disease modeling using adipose stem cells. *Eur J Endocrinol*. 2021;184(1):155-168. https://doi.org/10.1530/EJE-20-1013
22. Auclair M, Vigouroux C, Desbois-Mouthon C, *et al*. Antiinsulin receptor autoantibodies induce insulin receptors to constitutively associate with insulin receptor substrate-1 and -2 and cause severe cell resistance to both insulin and insulin-like growth factor I. *J Clin Endocrinol Metab*. 1999;84(9):3197-3206. https://doi.org/10.1210/jcem.84.9.5965
23. Mandato C, Siano MA, Nazzaro L, *et al*. A ZFYVE19 gene mutation associated with neonatal cholestasis and cilia dysfunction: case report with a novel pathogenic variant. *Orphanet J Rare Dis*. 2021;16(1):179. https://doi.org/10.1186/s13023-021-01775-8
24. Karhan AN, Zammouri J, Auclair M, *et al*. Biallelic CAV1 null variants induce congenital generalized lipodystrophy with achalasia. *Eur J Endocrinol*. 2021;185(6):841-854. https://doi.org/10.1530/EJE-21-0915
25. Richards S, Aziz N, Bale S, *et al*. Standards and guidelines for the interpretation of sequence variants: a joint consensus recommendation of the American College of Medical Genetics and Genomics and the Association for Molecular Pathology. *Genet Med*. 2015;17(5):405-424. https://doi.org/10.1038/gim.2015.30
26. Koparir A, Karatas OF, Yuceturk B, *et al*. Novel POC1A mutation in primordial dwarfism reveals new insights for centriole biogenesis. *Hum Mol Genet*. 2015;24(19):5378-5387. https://doi.org/10.1093/hmg/ddv261
27. Ko JM, Jung S, Seo J, *et al*. SOFT syndrome caused by compound heterozygous mutations of POC1A and its skeletal manifestation. *J Hum Genet*. 2016;61(6):561-564. https://doi.org/10.1038/jhg.2015.174
28. Barraza-García J, Iván Rivera-Pedroza C, Salamanca L, *et al*. Two novel POC1A mutations in the primordial dwarfism, SOFT syndrome: clinical homogeneity but also unreported malformations. *Am J Med Genet Part A*. 2016;170(1):210-216. https://doi.org/10.1002/ajmg.a.37393
29. Mostofizadeh N, Gheidarloo M, Hashemipour M, Dehkordi EH. SOFT syndrome: the first case in Iran. *Adv Biomed Res*. 2018;7(1):128. https://doi.org/10.4103/abr.abr_13_18
30. Saida K, Silva S, Solar B, *et al*. SOFT syndrome in a patient from Chile. *Am J Med Genet Part A*. 2019;179(3):338-340. https://doi.org/10.1002/ajmg.a.61015
31. Li S, Zhong Y, Yang Y, He S, He W. Further phenotypic features and two novel POC1A variants in a patient with SOFT syndrome: a case report. *Mol Med Rep*. 2021;24(1):494. https://doi.org/10.3892/mmr.2021.12133
32. Homma TK, Freire BL, Honjo Kawahira RS, *et al*. Genetic disorders in prenatal onset syndromic short stature identified by exome sequencing. *J Pediatr*. 2019;215:192-198. https://doi.org/10.1016/j.jpeds.2019.08.024
33. Al-Kindi A, Al-Shehhi M, Westenberger A, *et al*. A novel POC1A variant in an alternatively spliced exon causes classic SOFT

syndrome: clinical presentation of seven patients. *J Hum Genet*. 2020;65(2):193-197. https://doi.org/10.1038/s10038-019-0693-2
34. Zhu D, Shi S, Wang H, Liao K. Growth arrest induces primary-cilium formation and sensitizes IGF-1-receptor signaling during differentiation induction of 3T3-L1 preadipocytes. *J Cell Sci*. 2009;122(15):2760-2768. https://doi.org/10.1242/jcs.046276
35. Dalbay MT, Thorpe SD, Connelly JT, Chapple JP, Knight MM. Adipogenic differentiation of hMSCs is mediated by recruitment of IGF-1r onto the primary cilium associated with cilia elongation. *Stem Cells*. 2015;33(6):1952-1961. https://doi.org/10.1002/stem.1975
36. Yamakawa D, Katoh D, Kasahara K, *et al*. Primary cilia-dependent lipid raft/caveolin dynamics regulate adipogenesis. *Cell Rep*. 2021;34(10):108817. https://doi.org/10.1016/j.celrep.2021.108817
37. Wang L, Liu Y, Stratigopoulos G, *et al*. Bardet-Biedl syndrome proteins regulate intracellular signaling and neuronal function in patient-specific iPSC-derived neurons. *J Clin Investig*. 2021;131(8):e146287. https://doi.org/10.1172/JCI146287
38. Silva DF, Cavadas C. Primary cilia shape hallmarks of health and aging. *Trends Mol Med*. 2023;29(7):567-579. https://doi.org/10.1016/j.molmed.2023.04.001
39. Cutfield WS, Wilton P, Bennmarker H, *et al*. Incidence of diabetes mellitus and impaired glucose tolerance in children and adolescents receiving growth-hormone treatment. *Lancet*. 2000;355(9204):610-613. https://doi.org/10.1016/S0140-6736(99)04055-6
40. Sharma R, Kopchick JJ, Puri V, Sharma VM. Effect of growth hormone on insulin signaling. *Mol Cell Endocrinol*. 2020;518:111038. https://doi.org/10.1016/j.mce.2020.111038
41. Guo DF, Lin Z, Wu Y, *et al*. The BBSome in POMC and AgRP neurons is necessary for body weight regulation and sorting of metabolic receptors. *Diabetes*. 2019;68(8):1591-1603. https://doi.org/10.2337/db18-1088
42. Wang Y, Bernard A, Comblain F, *et al*. Melanocortin 4 receptor signals at the neuronal primary cilium to control food intake and body weight. *J Clin Investig*. 2021;131(9):e142064. https://doi.org/10.1172/JCI142064
43. Zhang Y, Hao J, Tarrago MG, *et al*. FBF1 deficiency promotes beiging and healthy expansion of white adipose tissue. *Cell Rep*. 2021;36(5):109481. https://doi.org/10.1016/j.celrep.2021.109481
44. Geister KA, Brinkmeier ML, Cheung LY, *et al*. LINE-1 mediated insertion into Poc1a (protein of centriole 1 A) causes growth insufficiency and male infertility in mice. *PLoS Genet*. 2015;11(10):e1005569. https://doi.org/10.1371/journal.pgen.1005569
45. Semple RK, Cochran EK, Soos MA, *et al*. Plasma adiponectin as a marker of insulin receptor dysfunction: clinical utility in severe insulin resistance. *Diabetes Care*. 2008;31(5):977-979. https://doi.org/10.2337/dc07-2194